# department of chemical engineering and fuel technology

UNIVERSITY OF SHEFFIELD

(2)

# SPRAY EVAPORATION IN RECIRCULATING FLOW

F. BOYSON AND J. SWITHENBANK

Dept. of Chemical Engineering and Fuel Technology, Sheffield University.

Paper for 17th International Symposium, on Combustion. Leeds 1978.

H1C 290 April, 1978

# Spray Evaporation in Recirculating Flow

F. Boyson* and J. Swithenbank

Department of Chemical Engineering and Fuel Technology,

Sheffield University.

## Summary

Since the overall rate of fuel evaporation in combustors is strongly influenced by the gas:drop relative velocity, detailed information on the aerodynamics of the flow in a given combustor configuration is essential for its prediction. Such aerodynamic information can be obtained either from measurements or from mathematical simulation of the events taking place in actual systems. Owing to the advances made in the field of mathematical modelling turbulent flow phenomena, and the development of powerful techniques for solving the partial differential equations of fluid mechanics, the latter approach is on the way to becoming more efficient and economical. The flow equations can be solved using either two or three dimensional models, however, almost all practical systems may be treated as two-dimensional (axisymmetric) in the important region, which includes the region of soot formation near the fuel injector.

The calculation procedure is here applied to the case of fuel injection into a recirculation zone behind a baffle in a duct. The elliptic flow equations are evaluated using the k,ε model of turbulence. The simultaneous differential equations of droplet dynamics are evaluated in each cell of the flowfield for each size group of the spray using short time steps. To adequately represent the typical fuel spray size distributions, twenty size intervals of droplets are required.

The results clearly demonstrate the controlling influence of the convective contribution to spray evaporation. A particularly interesting conclusion of the analysis is that, in conditions representative of

combustion systems, the droplets have just deviated from their initial conical path towards the flow direction when they vanish. This phenomena is consistent with experimental observations and to a great extent justifies the use of two-dimensional modelling for the spray evaporation region of practical combustors.

* Present Address

I. T. U. Makina Fakültesi,

Motordar Kursusu,

Gumussuyu,

Istanbul,

TURKEY.

## 1. Introduction

At the present time about one half of the World's fossil fuel production is consumed through spray combustion. The accurate prediction of the combustion behaviour of fuel sprays increases the designers ability to optimize the design of gas turbine and industrial combustors, diesel engines, etc., to improve efficiency and minimize pollutant production.

In the past there have been many studies on the vaporization of single droplets (eg. Ref. 1), and a smaller number of studies have been concerned with the combustion of clouds of droplets (eg Ref. 2). In Refs 3 & 4 it shown that in most practical combustors the flame does not generally stabilize on the individual droplets, but the droplets first evaporate, then the fuel mixes with the air, and combustion actually occurs in a turbulent mixing controlled flame. This does not mean that evaporation does not play a part in determining the combustor characteristics. Indeed, Fig 1 shows that the measured stability loops for a small gas turbine combustor vary dramatically with the fuel nozzle rating i.e. droplet size distribution[5]. This figure clearly demonstrates that the finer fuel spray (resulting from a nozzle with a smaller flow rating) gives a greater proportion of the fuel evaporated and mixed in the flame stabilizing primary zone of the combustor.

Recent experimental studies have shown that the proportion of pollutants produced by gas turbine combustors may be minimized by the use of pre-mixed, pre-vapourized fuel. In Ref 6 for example, it is shown that pre-vapourizing the fuel decreased the production of CO, $NO_x$ and smoke number by 30%, 24% and 60% respectively. Pre-mixed

pre-vapourized combustors operating with lean primary zones have achieved $NO_x$ levels down to 0.3g $NO_2$/kg fuel at the supersonic cruise condition[7], and they are likely to be suitable for future synthetic fuels having a low H/C ratio. A carburation system capable of providing a uniformly pre-mixed, pre-vapourized fuel is described in Ref 8. There is thus considerable current interest in predicting the detailed overall behaviour of combustion systems with various methods of fuel preparation. In order to predict quantitatively the characteristics (ie. stability, efficiency and pollutant production) of a combustor, we must calculate both the path of the various drop sizes in the spray, and the distribution of the fuel evaporated from the spray. In current gas turbine combustors, as in many other applications of spray combustion, the droplets evaporate along their trajectories in the presence of a forced convective motion of the gas, leaving behind pockets of fuel vapour which later mix with the oxidizer and burn. While smaller droplets evaporate almost instantaneously, larger ones may penetrate the flamefront depending on the compromise between the degree of atomization of the liquid spray and its issue velocity. Since the overall rate of evaporation is very strongly influenced by the gas-drop relative velocity, detailed information on the aerodynamics of the flow in a given combustor configuration is essential for its prediction. Such information can be obtained either from measurements or from simulation of the events taking place in actual systems. Owing to the advances made in the field of mathematically modelling turbulent flow phenomena[9] and the development of powerful techniques for solving the partial differential equations of fluid mechanics[10], the latter approach is on the way to becoming more efficient and economical.

The flow equations can be solved using either two or three dimensional models[11], however the solution of the three dimensional, two phase equations require considerable computer time as is shown in Ref 12. In practical combustors, the region in the general vicinity of the fuel injector is of particular concern, since this is the region where soot may be formed from unburned fuel if the mixtures are locally rich. (The mechanism of soot formation is discussed in Ref. 13 where equations are given for both the first stage representing the formation of radical nuclei, and the second stage representing soot particle formation from these nuclei). Fig. 2 shows the flow pattern in the primary zone of a simple gas turbine combustor, computed by 3-dimensional mathematical modelling[12] and it can be seen that the flow is effectively 2-dimensional in the region of the fuel injector. It will be shown below that the fuel trajectory lies in this region and hence 2-dimensional modelling of the spray evaporation is justified.

The main purpose of the present study is to demonstrate a technique for predicting the rate of evaporation of the fuel spray by combining the abovementioned methods of handling turbulent flow situations with spray dynamics. The basic approach is to determine the flowfield first, and then proceed to the calculation of the trajectories of individual droplets, the droplet velocities along these trajectories, the change of size distribution and finally the rate of evaporation.

Separate calculations (to be published) have shown that at conditions in typical gas turbine and industrial combustors, the influence of the droplets on the flowfield is negligable except in the initial region of spray break-up. This interaction only becomes significant when the droplet velocities are an order of magnitude greater than the gas velocity.

This condition sometimes arises when fuel is injected into a recirculating flow of particularly low velocity, but is unimportant for the cases discussed herin. The current trend towards air blast atomizers and other devices producing fine sprays implies that the interaction will continue to be negligable for most practical combustors.

To demonstrate the method, the calculation procedure is applied to the case of injection into a recirculation zone behind a circular baffle in a duct. The governing equations of the fluid flow together with the turbulence model employed and the method of solution are described in Section 2. Section 3 deals with some aspects of spray evaluation and the results are presented in Section 4. In Section 5 the results of various experimental tests are interpreted in terms of the theoretical predictions.

## 2. The Theoretical Formulation

In the absence of heat and mass transfer and chemical reactions the governing equations of the flow are the well established equations for the conservation of mass and momentum, supplemented by the equations of the kinetic energy of turbulence and the rate of dissipation of energy, which constitute a simultaneous nonlinear set. In the case of two dimensional and axially symmetric flow problems it is advantageous to work with vorticity and stream function as the dependent variables rather than the components of velocity and pressure. The advantages exhibit themselves in the elimination of pressure from the equations and the reduction of the total number of equations to be solved from five to four. The primitive variables are recovered after the solution of the problem is established.

The general form of the equations in cylindrical coordinates, as given by Gosman et. al.[10] is the following:

$$a_\phi\left[\frac{\partial}{\partial x}\left(\phi\frac{\partial\psi}{\partial y}\right) - \frac{\partial}{\partial y}\left(\phi\frac{\partial\psi}{\partial x}\right)\right] - \frac{\partial}{\partial x}\left[b_\phi y\frac{\partial}{\partial x}(c_\phi\phi)\right] - \frac{\partial}{\partial y}\left[b_\phi y\frac{\partial}{\partial y}(c_\phi\phi)\right] + y^2 d_\phi = 0 \quad . \tag{1}$$

Here, $\phi$ is the general dependent variable which can stand for vorticity divided by the distance from the axis of symmetry $\omega/y$, the stream function $\psi$, the kinetic energy of turbulence k, and the rate of energy dissipation $\varepsilon$. The corresponding expressions for the quantities $a_\phi$, $b_\phi$, $c_\phi$ and $d_\phi$ are given in Table 1.

| $\phi$ | $a_\phi$ | $b_\phi$ | $c_\phi$ | $d_\phi$ |
|---|---|---|---|---|
| $\omega/y$ | $y^2$ | $y^2$ | $\mu_{eff}$ | 0 |
| $\psi$ | 0 | $1/\rho y^2$ | 1 | $-\omega/y$ |
| k | 1 | $\mu_{eff}/\sigma_{k,eff}$ | 1 | $-G + C_D\rho\varepsilon$ |
| $\varepsilon$ | 1 | $\mu_{eff}/\sigma_{\varepsilon,eff}$ | 1 | $C_1 G\varepsilon/k + C_2\rho\varepsilon^2/k$ |

$$G = \mu_{eff}\left[2\left(\left\{\frac{\partial u}{\partial x}\right\}^2 + \left\{\frac{\partial v}{\partial y}\right\}^2 + \left\{\frac{v}{y}\right\}^2\right) + \left(\frac{\partial u}{\partial y} + \frac{\partial v}{\partial x}\right)^2\right]$$

Table 1. Expressions for quantities appearing in eq. (1).

The effective viscosity is the sum of laminar viscosity and a turbulent counterpart originating from the mixing length hypothesis. The turbulent viscosity is linked to the kinetic energy of turbulence and the energy dissipation rate in the following fashion:

$$\mu_t = C_\mu \rho k^2/\varepsilon \qquad (2)$$

Here, $\rho$ is the density of the fluid and $C_\mu$, $C_D$, $C_1$, $C_2$ $\sigma_{k,eff}$ and $\sigma_{\varepsilon,eff}$ are constants, the recommended values[14] for which are given in Table 2.

| $C_\mu$ | $C_D$ | $C_1$ | $C_2$ | $\sigma_{k,eff}$ | $\sigma_{\varepsilon,eff}$ |
|---|---|---|---|---|---|
| 0.09 | 1.0 | 1.44 | 1.92 | 1.0 | 1.21 |

Table 2. Recommended values of the constants of the turbulence model (14).

The details of placing the general partial differential equation (1) into finite difference form by integrating it over a control volume is given by Gosman et.al.[10]. A typical control volume and associated symbols are shown in Figure 3. The successive substitution formula which can stand for either of the dependent variables is of the following form:

$$\phi_P = C_E\phi_E + C_W\phi_W + C_N\phi_N + C_S\phi_S + S, \qquad (3)$$

where the C's are the coefficients which contain contributions from the convective and diffusive fluxes and S is the source term. Due to the elliptic nature of the equations, the successive substitution formula must be supplemented by boundary conditions specified at all boundaries. Attention shall now be directed towards the specification of boundary conditions relevant to the baffle problem at hand.

The geometry of the domain of integration is shown in Figure 4. Four different types of boundary can be distinguished: the inlet, the walls, the axis of symmetry and the exit. The conditions at these boundaries will be handled separately.

*Inlet.* The conditions at the inlet are specified once and for all. In other words the values of the dependent variables are fixed there and do not require updating during the iteration process.

*Wall Boundaries.* The stream function does not present difficulties and its value is constant along the walls. However, it is known from practice that steep gradients of transport properties and other dependent variables occur near the walls in turbulent flow. To avoid fine grids and excessive computing time use is made of the

wall flux relations near the walls. The familiar log-law of the wall can be stated as:

$$u_\tau = \kappa u_p \left( \log_e (E\, n u_\tau \rho / \mu) \right)^{-1} \quad , \qquad (4)$$

where, $\mu$ is the laminar viscosity, $\rho$ is the fluid density, n is the normal distance from the wall, $u_p$ is the streamwise velocity at a point near the wall, $u_\tau$ is the 'shear velocity' and, E and $\kappa$ are constants whose values are 9.793 and 0.4187 respectively. The boundary conditions for all the dependent variables except the stream function are derived from equation (4) with the assumption that the flow is essentially one dimensional in the vicinity of the walls. These conditions are specified at next to wall grid points.

*Axis of Symmetry.* The stream function must be constant along the axis of symmetry and its value is usually taken as zero. Also, it is obvious that the normal derivatives of k and $\varepsilon$ must vanish on the axis. On the other hand, although the vorticity itself is zero the same is not valid for $\omega/y$. A satisfactory boundary condition for this variable can be derived by expanding $\psi$ into a power series in y for constant x in the immediate neighbourhood of the axis and substituting this into the definition of vorticity. This treatment leads to the conclusion that the normal derivative of $\omega/y$ is also zero at y equals zero.

*Exit.* Since the distributions of the dependent variables at the exit plane are not known beforehand, it is necessary to employ gradient type boundary conditions there. This is expressed mathematically as $\partial\phi/\partial x = 0$.

The set of simultaneous linear equations together with the algebraic relationships which define the conditions at the boundaries are solved using the Gauss-Seidel iterative scheme. To suppress divergence provoked by large variations in the source terms of the successive substitution formula (3 ), k, $\varepsilon$ and $\mu$ are underrelaxed. The underrelaxation factors for the kinetic energy of turbulence k and the energy dissipation rate $\varepsilon$ are set at 0.7, and that of turbulent viscosity at 0.5. Other variables do not require underrelaxation.

The iteration process is terminated when the maximum percentage change of all dependent variables in successive iterations falls below $10^{-4}$.

## 3. Spray Evaluation

Once the flow field is established by the methods described in the previous sections, the next step is the determine the time rate of evaporation of a fuel spray into this field at a given point. (N.B. Alternatively the flowfield could be determined experimentally).

The equation of motion of a droplet in the absence of all external forces except drag is:

$$\frac{d\vec{u}_p}{dt} = -\frac{3}{4}\frac{\rho_g}{\rho_l}\frac{C_D}{D}(\vec{u}_p - \vec{u})|\vec{u}_p - \vec{u}| \qquad (5)$$

where $\vec{u}_p$ and $\vec{u}$ are the absolute droplet and gas velocities respectively, t is the time, $\rho_l$ is the liquid density, $\rho_g$ is the gas density, $C_D$ is the drag coefficient and D is the droplet diameter. When written in component form this becomes,

$$\frac{du_p}{dt} = -\frac{3}{4}\frac{\mu}{\rho_l D^2} C_D \, Re \, (u_p - u) \qquad (6)$$

for the x-direction, and

$$\frac{dv_p}{dt} = -\frac{3}{4}\frac{\mu}{\rho_l D^2} C_D \, Re \, (v_p - v) \qquad (7)$$

for the y-direction. Here $\mu$ is the viscosity of the gas and Re is the relative Reynolds number defined as follows:

$$Re = D\rho_g|\vec{u}_p - \vec{u}|/\mu \, .$$

If the droplet is evaporating a third equation giving the rate of change of its diameter with respect to time is needed. In the case of forced convective evaporation this can be written as,

$$\frac{dD}{dt} = -\frac{C_b}{2D}\left(1 + 0.23\, Re^{1/2}\right) . \qquad (8)$$

$C_b$ is the evaporation rate constant whose value depends on the type of fuel as well as the properties and temperature of the surrounding medium. A widely used expression for $C_b$ derived from the quasi-steady analysis of droplet combustion is that given by Wise and Agoston[15]:

$$C_b = \frac{8\lambda}{\rho_l c_p} \log_e\{1 + \frac{c_p}{L}(T_\infty - T_l)\} \qquad (9)$$

where, $\lambda$ and $c_p$ are the thermal conductivity and the specific heat at constant pressure of the surrounding gas, L is the latent heat of evaporation, $T_\infty$ and $T_l$ are the ambient and drop surface temperatures respectively. This equation shows that the evaporation constant is strongly influenced by the properties of the gas, $\lambda/c_p$, and that it depends logarithmically on the heat of vapourization and temperature.

Equations (6), (7) and (8) constitute a set of simultaneous ordinary differentials equations which are supplemented with the auxilliary relations for the evaporation rate constant and the drag coefficient, and subject to a given set of initial conditions. The components of gas velocity needed for the solution of these equations are recovered from the distribution of the stream function and are specified at the grid nodes. Since the distrubutions of these are not available as continuous function of x and y, it is assumed that u and v are uniform within the cells and that their values are the same as those prevailing at point P which the cell encloses. An alternative but probably time consuming approach would be to express u and v as analytical functions by a least squares fit or any other similar process.

Focusing attention on the translation of a droplet in a given cell and considering only a very short segment of its trajectory, it can be stipulated that the quantities $C_D Re$ and $(1 + 0.23\ Re^{1/2})$

vary only negligibly throughout that segment. It is then possible to integrate equations (6), (7) and (8) analytically. However, it must be remembered that the solutions thus obtained are only valid if the time increment under consideration is sufficiently small. Integration of equation (8) gives,

$$D^2 = D_0^2 - C_b(1 + 0.23\ Re^{1/2})(t - t_0) \tag{10}$$

for the time dependence of the droplet diameter. Re is the relative Reynolds number evaluated at time $t_0$. Substituting this into equations (6) and (7) and integrating,

$$u_p = u + (u_{p,0} - u)(D/D_0)^{2\alpha} \tag{11}$$

and

$$v_p = v + (v_{p,0} - v)(D/D_0)^{2\alpha}$$

with

$$\alpha = \frac{3}{4}\frac{\mu}{\rho_l}C_D Re\left(C_b(1 + 0.23\ Re^{1/2})\right)^{-1} \tag{12}$$

are obtained for the components of the droplet velocity. The coordinates of the instantaneous location of the drop are recovered by integrating these with respect to time. Giving,

$$x = x_0 + (t - t_0)u - \frac{D_0^2}{\beta}(u_{p,0} - u)\left(\left(\frac{D}{D_0}\right)^{2(\alpha+1)} - 1\right) \tag{13}$$

and

$$y = y_0 + (t - t_0)v - \frac{D_0^2}{\beta}(v_{p,0} - v)\left(\left(\frac{D}{D_0}\right)^{2(\alpha+1)} - 1\right) \tag{14}$$

with

$$\beta = C_b(1 + 0.23\ Re^{1/2})(1 + \alpha)\ .$$

The set of equations (11), (12), (13) and (14), which give the velocity and the location of a droplet of diameter D at a given instant of time, must be supplied with the relationship between the drag coefficient and the relative Reynolds number. The three point formula of Morsi and Alexander[16] has been employed for the evaluation of the drag coefficient. This formula is expressed as,

$$C_D = \frac{K_1}{Re} + \frac{K_2}{Re^2} + K_3 \qquad (15)$$

where $K_1$, $K_2$ and $K_3$ are constants the values of which depend on the working range of Reynolds number.

Since the spray is made up of a spectrum of droplet sizes, information on the initial size distribution is also required for the estimation of the rate of its evaporation. This information is normally obtained from measurements. An extremely rapid and simple method which can be used for determining the size distribution in terms of the Rosin-Rammler parameters is the laser diffraction technique of Swithenbank et. al.[17]. Owing to its simplicity the Rosin-Rammler equation has been employed in this study, however other functions such as the Nukiyama-Tanasawa or the log-normal distributions can be accomodated when required.

The calculation procedure is further facilitated if the distribution curve is divided into an adequate number of size groups each represented by a mean diameter D. The initial mass fraction of each group can then be expressed as,

$$\Delta m = \rho_l \frac{\delta D^{\delta-1}}{\bar{D}^{\delta}} \exp\{-(D/\bar{D})^{\delta}\}\ \Delta D \qquad (16)$$

where $\Delta m$ is the mass of drops of size $\pm\Delta D/2$ around $D$ per unit volume of injected fuel, $\bar{D}$ is the size constant and $\delta$ is the distribution parameter. Normally 15 to 20 size intervals are required to represent the spray adequately. For each size range the following steps are performed at every time increment:

1. The relative Reynolds number is calculated using the conditions prevailing at the beginning of the increment denoted by time t.
2. The drag coefficient $C_D$ is obtained from the three point formula and the quantities $C_D Re/24$ and $(1 + 0.23\ Re^{1/2})$ are formed.
3. The drop diameter at time $t+\Delta t$ is calculated from equation 10.
4. The mass remaining at $t+\Delta t$ is found from

$$\Delta m_{t+\Delta t} = \Delta m_t \left( D_{t+\Delta t}/D_t \right)^3$$

5. The new values of u and v are calculated from equations 11. These are required to determine the quantities involving the Reynolds number for the next increment of time.
6. The location of the droplet at time $t+\Delta t$ is obtained from equations 14. This location is checked against the cell boundaries to find out whether the drop has moved into one of the neighbouring cells. If so the corresponding values of the components of air velocity are substituted in equations 13 and 14.

7. Steps 1 to 6 are repeated until the drop diameter falls to zero or impingement on wall boundaries occurs.

Once the evaporation histories of individual size groups are calculated the mass fractions are summed at predetermined instances to obtain the total evaporation time curves. It can be noted that the above formulation also yields drop trajectories, the drop velocity histories along these trajectories and the size distribution curves at different times.

## 4. Results

The calculations are performed for the geometry of an existing model combustor can of internal diameter 8 cms. and length 24 cms.. The baffle which is situated at the inlet is hemispherical in shape, its diameter being half that of the can. The air inlet velocity was taken as 10 m/sec.

Figurue 5. shows the streamlines of the mean flow in the recirculation zone and the development of the axial velocity distribution. It can be seen that the bubble extends to about one baffle diameter. The inspection of the velocity profiles reveals that the velocities in the recirculation zone are an order of magnitude smaller than those in the annular jet. Generally, these results agree at least qualitatively with experiment. The distribution of the kinetic energy of turbulence in the wake is given in Figure 6. The conclusion can be drawn that the level of turbulence exhibits a maximum in the latter part of the bubble. Again, these results show a qualitative agreement with the experimental findings of Davies and Beer,[18] although the two cases are not entirely similar.

The injected spray has been taken to have a total cone angle of $45^{o}$. All the droplets were assumed to leave the nozzle with an initial velocity of 21 m/sec. The calculations were performed for two different size constants of the Rosin-Rammler distribution, 50 and 100 microns, and the distribution parameter was set at 2. The values of the evaporation constant worked out from equation (9) for $T_{\infty} = 1500^{o}K$ and $\lambda/c_p = 7.8 \times 10^{-4}$ grms./cm-sec range from 0.002 to 0.01 $cm^2$/sec depending on the properties of the fuel. Since the effect of the oxidizer mass fraction is omitted in equation (9),

these are lower than the corresponding burning rate constants. An overall value of 0.005 $cm^2/sec$ has been used throughout the present calculations.

The trajectories of individual droplets are presented in Figure 7. These show a slight deviation from the nominal cone in the recirculation region and bend thereafter towards the downstream direction. It can be seen that the smaller droplets evaporate completely in the vicinity of the point of issue, whereas those with initial diameters larger than 110 microns hit the wall of the duct. Figures 8 and 9 show the profiles of unevaporated mass fraction against time for two different values of the size constant. As expected, forced convection has an appreciable influence on the rate of evaporation. Again, both figures show that this rate increases with decreasing size constant. Figure 10 gives the change of the distribution function with time for $\bar{D}$ = 100 microns. The peak of the curve shifts to the right as time elapses.

## 4.1 Heat Transfer to Droplets

The evaporation lag of droplets which is defined as the time required to bring the surface temperature of a droplet to the boiling point of liquid is considered. The time rate of change of the droplets temperature is given by

$$\frac{dT}{dt} = \frac{6\ Nu\ k}{\rho_1 D^2 c_{p,d}} (T_\infty - T)$$

where, k is the thermal conductivity of the gas, Nu the Nusselt number, $c_{p,d}$ the specific heat of droplets and $T_\infty$ the temperature of the surrounding medium. Under forced convective motion the Nusselt number is given by the following equation which is due to Ranz and Marshall,

$$Nu = 2 + 0.6\ Re^{.5}\ Pr^{.333}$$

where, RE is the relative Reynolds number and Pr is the Prandtl number. Supposing T is constant throughout, the above equation can be integrated to give

$$T = T_\infty - (T_\infty - T_o)\ e^{-(6\ Nu\ k\ t/\rho_1 D^2 c_{p,d})}$$

where, $T_o$ is the initial droplet temperature and D is its diameter. A calculation has been performed with $T = 1500^oK$, $T_o = 320^oK$, $k = 10^{-3}$ W/cm $^oK$, $c_{p,d} = 3$ Ws/gr $^oK$ the results of which are presented in Figs 11 & 12. The boiling point of fuel was taken to be $450^oK$.

## 5. Discussion.

The results presented above predict several significant features. In the hot combustion environment sprays of the type commonly used in combustors tend to travel in near straight lines. The smaller droplets < 50 μm typically only travel 2 - 3 centimetres before evaporating away, whereas droplets greater than 100 μm travel many centimetres and may hit the combustor wall. In general, as a droplet becomes small enough to be deflected by the gas flow, its life is so short that it quickly vanishes. This conclusion is also true when allowance is made for the heating-up time of the drop as this factor only contributes about 10% to the range. These results account for the experimental observations at Sheffield University, (Chigier et al[19]) in which very detailed measurements were made of the streamlines, droplet 'trajectories', temperatures and concentrations in a flame stabilised behind a disc furnished with a hollow cone spray nozzle of $41^{o}$ total cone angle. The overall spray model deduced in Ref 19 is reproduced in Fig. 13. In the photographic method used, it is difficult to follow the time history of individual droplets since their size changes continuously as they evaporate. Nevertheless the experimental results clearly show that in the hot environment, droplets larger than 100 μm move in straight lines, whilst as they near the end of their life they tend to align with the local streamlines. In the cold unburning environment the drag on the particles is much larger and their lifetimes are much longer. Consequently, small droplets may be captured in the turbulent recirculation zone and are then observed moving in all directions in this region.

Flame stabilization behind a disc in a duct using a 90° cone angle liquid propane fuel spray has been studied at Perdue University[20]. Detailed concentration and temperature maps are presented from which the spray path and reaction zones are deduced. Again the results agree with the predictions of the analysis presented above, and the relationships established show how the evaporation rate can be related to pollutant formation in the various combustion zones.

Finally the fact that large droplets arrive at the predicted location on the walls of a gas turbine combustor can be experimentally demonstrated by simply inspecting the wall of the burning combustor using a very high intensity lamp to overcome the flame radiation. The intermittently wet surface spots may be readily seen.

Acknowledgements

Financial suport for this work from the Science Research Council and the USAF European Office of Aerospace Research Grant No. 74-2682C is gratefully acknowledged.

References


1. Ohta, Y., Shimoyama, K., and Ohigashi, S. 'Vaporization and Combustion of Single Liquid Fuel Droplets in a Turbulent Environment' Bulletin of the JSME Vol 18 No. 115 Jan 1975.

2. Williams, A., 'Combustion of Sprays of Liquid Fuels' Elek Science, London 1976.

3. Sjogren, A., 'Soot Formation by Combustion of an Atomized Liquid Fuel' Fourteenth Symposium (Intl) on Combustion. The Combustion Institute p 919 1972.

4. Chigier, N.A. and Yule, A.J., 'Vaporization of Droplets in High Temperature Gas Streams' Levich Birthday Conference, Oxford, July 1977.

5. Poll, I., Payne, R., Swithenbank, J. and Vincent, M.W. 'Combustor Modelling' Proceedings of the 2nd International Symposium on Air Breathing Engines, March 1974. Published by the Royal Aeronautical Society.

6. Jones, R.E. and Grobman, J. "Design and Evaluation of Combustors for Reducing Aircraft Engine Pollution, 41st Meeting of AGARD/ Propulsion and Energetics Panel, London April 1973.

7. Roffe , G. and Ferri, A. 'Effect of Premixing Quality on Oxides of Nitrogen in Gas Turbine Combustors' NASA CR-2657, Feb 1976.

8. Roffe , G. 'Development of a Catalytic Combustor Fuel/Air Carburation System' AFAPL-TR-77-19 March 1977.

9. Launder, B.E. and Spalding, D.B. 'Mathematical Models of Turbulence' Academic Press. London 1972.

10. Gosman, A.D., Pun, W.M. Runchal, A.K., Spalding, D.B. and Wolfstein, M. 'Heat and Mass Transfer in Recirculating Flows', Academic Press, London. 1969.

11. Felton, P.G., Swithenbank, J. and Turan, A. 'Progress in Modelling Combustors' Fifth International Symposium on Combustion Processes, Krakow, Sept. 1977. Published in Archives of Thermodynamics and Combustion Vol. 9 1978.

12. Swithenbank J., Turan A. and Felton P.G. 'Modelling of Spray Combustors' Proceedings of the SQUID meeting: Gas Turbine Combustor Design Problems. 30-31 May 1978 Perdue University, to be published as a SQUID Report DDC 1978.

13. Magnussen B.F and Hertager, B.H. 'On Mathematical Modelling of Turbulent Combustion with Special Emphasis on Soot Formation and Combustion' 16th Symposium on Combustion, the Combustion Institute p 719 1977.

14. Jones, W.P. and Launder, B.E. 'The Prediction of Laminarization with a 2-equation Model of Turbulence 'Int J. Heat Mass Transfer 15, 301-314, 1972.

15. Wise, H. and Agoston, G.A. 'Literature on the Combustion of Petroleum' American Chemical Society, Washington D.C., 1958.

16. Morsi, S.A. and Alexander, A.J. 'An Investigation of Particle Trajectories in Two Phase Flow Systems' J. Fluid Mech. 55, 193-208, 1972.

17. Swithenbank, J., Beer, J.M., Taylor, D.S. Abbott, D. M$^{c}$Creath, G.C. 'A Laser Diagnostic Technique for the Measurement of Droplet and Particle Size Distributions', Experimental Diagnostics in Gas Phase Combustion Systems (Ed BT Zinn) Progess in Astonautics and Aeronautics Vol 53 p 421 - 448, 1977.

18. Davies, T.W. and Beér, J.M. 'The Turbulence Characteristics of Annular Wake Flow', Heat and Mass Transfer in Flows in Separated Regions, International Seminar, Hereig-Novi, Yugoslavia. 1969.

19. Chigier, N.A. and M$^{c}$Creath, C.G. 'Combustion of Droplets in Sprays' Acta Astonautica Vol 1 pp 687 - 710 1974.

20. Tuttle, J.H., Shisler, R.A. and Mellor, A.M. 'Investigation of Liquid Fueled Turbulent Diffusion Flames' Combustion Sci. & Tech. Vol. 14, pp. 229-241, 1976.

Fig. 1 Measured stability loops for 70 mm diam. gas turbine combustor.

Fig. 2. Axial and radial velocity distributions in primary zone of 70 mm diameter combustor.
a) In plane 10 mm downstream of fuel nozzle
b) In plane 6 mm upstream of primary jets.

Fig. 3 A Typical volume element.

Fig. 4 The domain of integration and boundary conditions

Fig. 5 The streamlines of the mean flow in the recirculation zone and axial velocity distributions at several downstream locations.

Fig. 6 Lines of equal turbulence kinetic energy in the wake.

Fig. 7 Trajectories of individual droplets. Arrows indicate burnout locations. Solid line is the nominal cone.

Fig. 8 Plots of unevaporated mass fraction against time, without forced convection ($\delta = 2$).

Fig. 9 Plots of unevaporated mass fraction against time, including forced convection ($\delta = 2$).

Fig.10 The change of distribution function for size constant, $\bar{D} = 100$ microns and distribution parameter $\delta = 2$ at $t = 0$.

Fig.11 Rate of evaporation with and without allowance for droplet heating up time.

Fig.12 Droplet trajectories with and without allowance for droplet heating-up time.

Fig.13 Physical model of spray burning in the wake of a stabilizer disc[19].

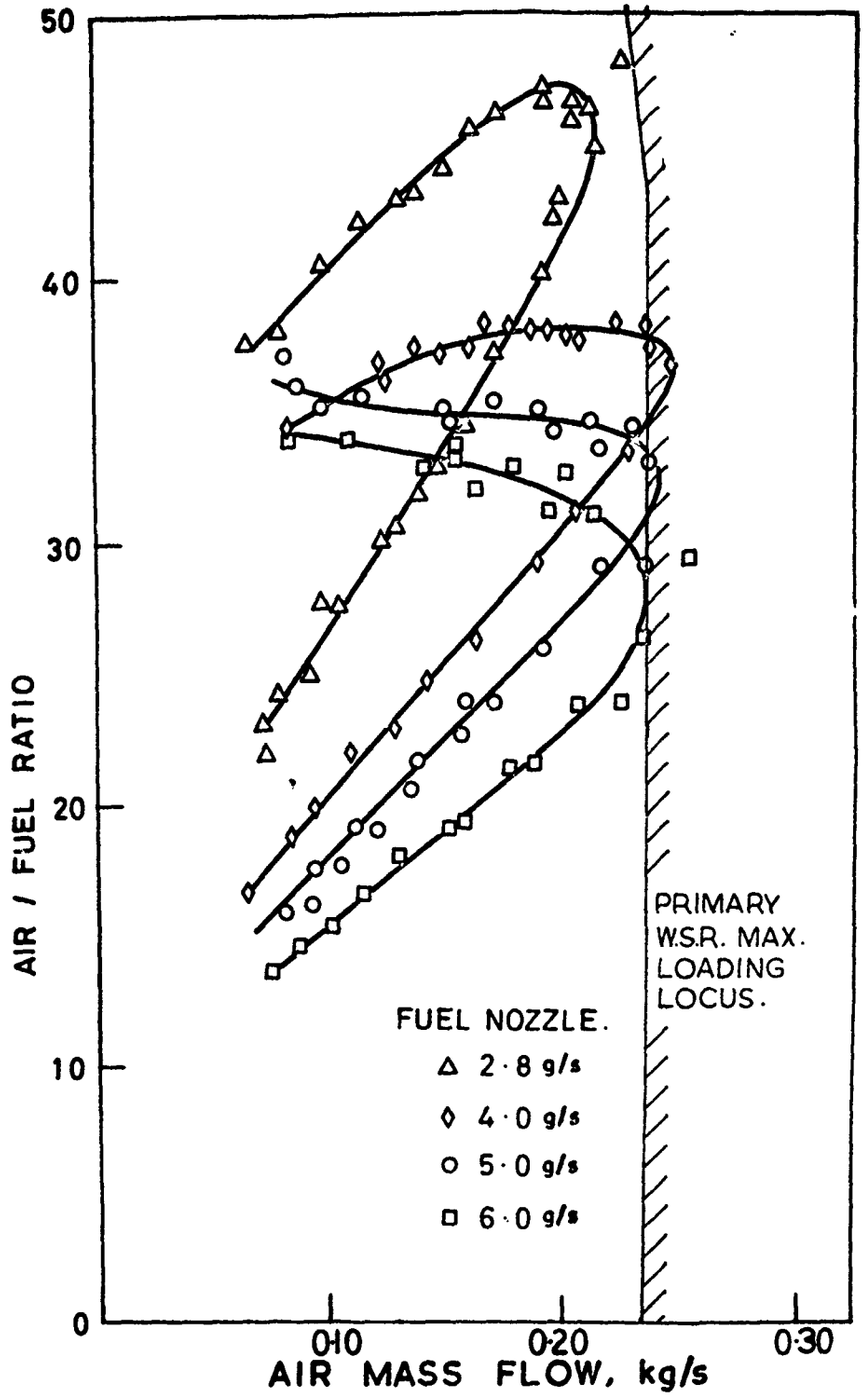


Fig. 1. Measured stability loops for 70 mm diam. gas turbine combustor

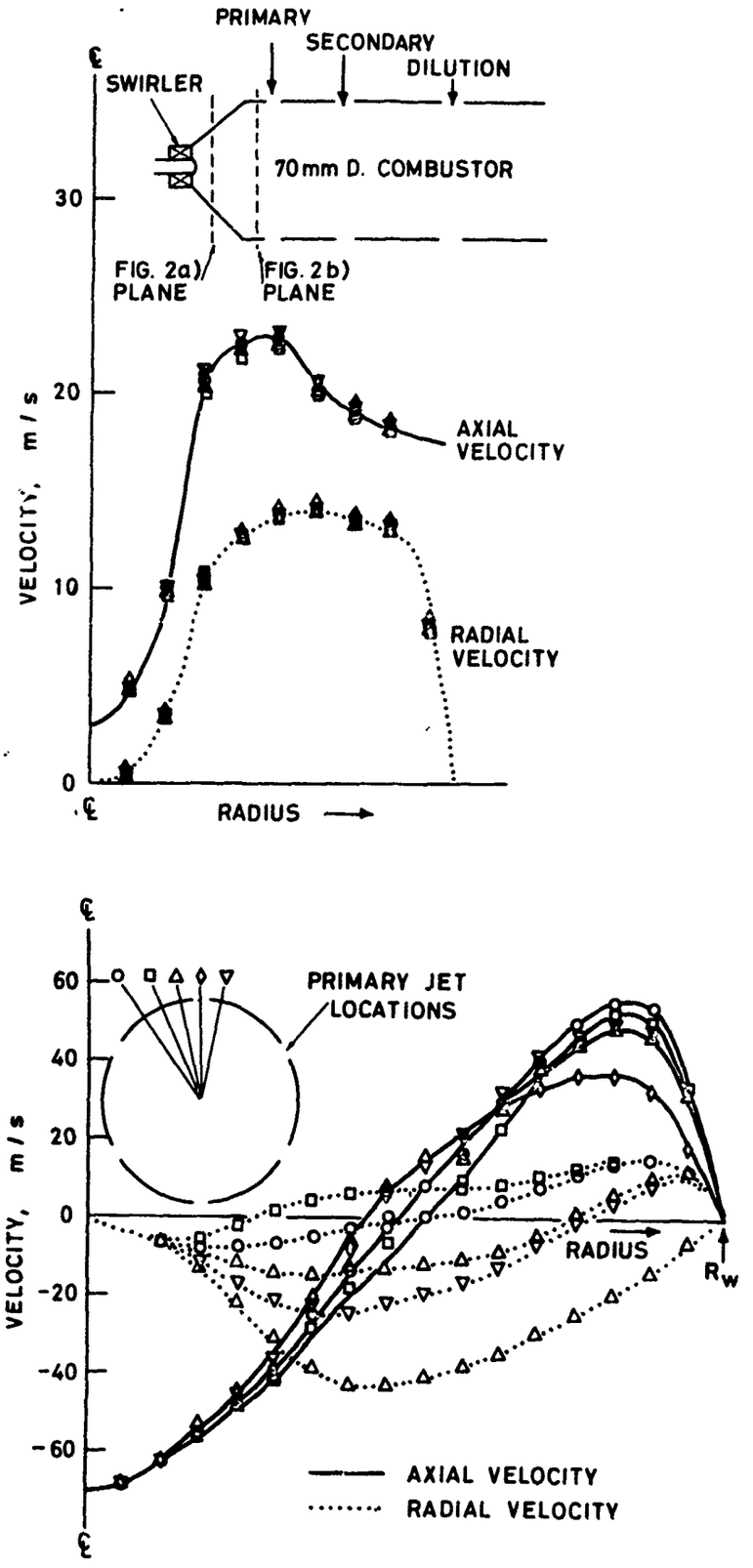


Fig. 2. Axial and radial velocity distributions in primary zone of 70 mm diameter combustor.

(a) In plane 10 mm downstream of fuel nozzle.

(b) In plane 6 mm upstream of primary jets.

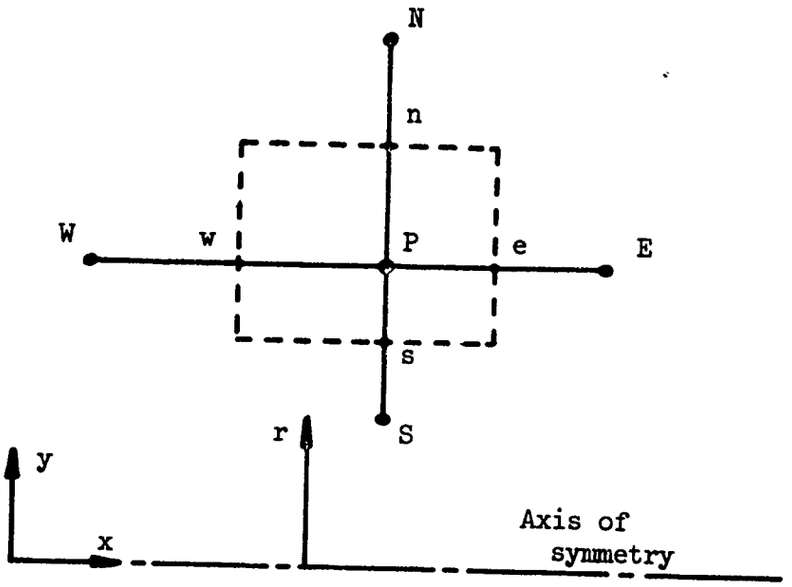


Fig. 3. A typical volume element.

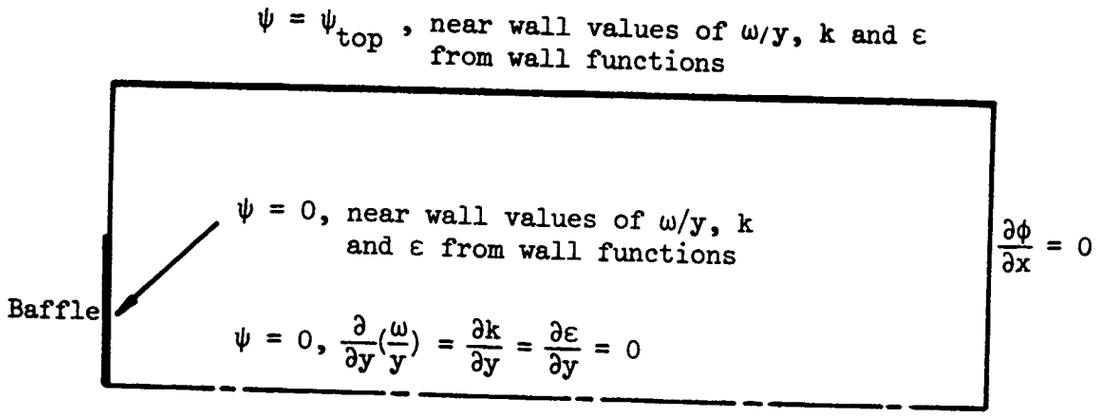


Fig. 4. The domain of integration and boundary conditions

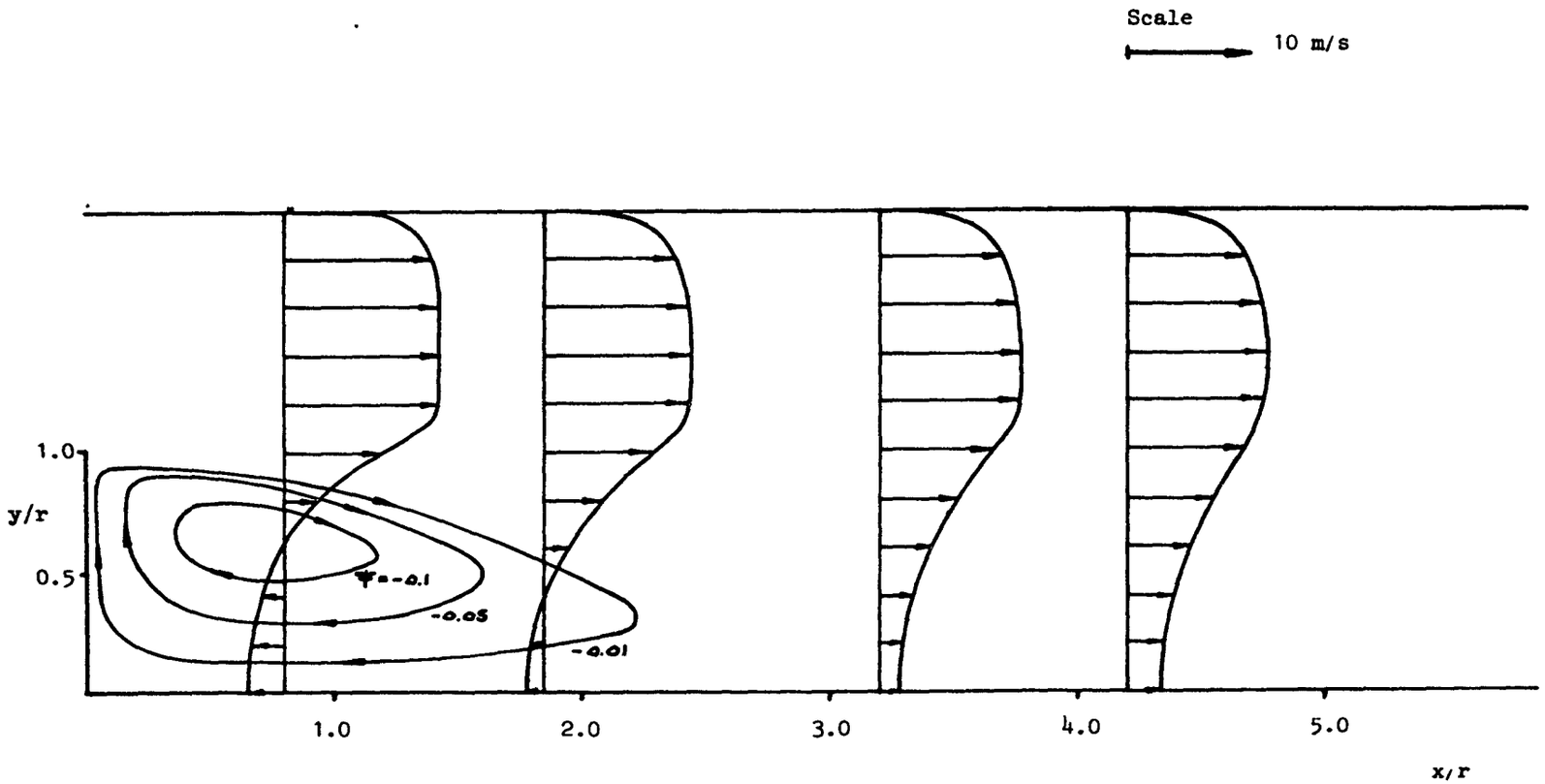


Fig. 5. The streamlines of the mean flow in the recirculation zone and axial velocity distributions at several downstream locations.

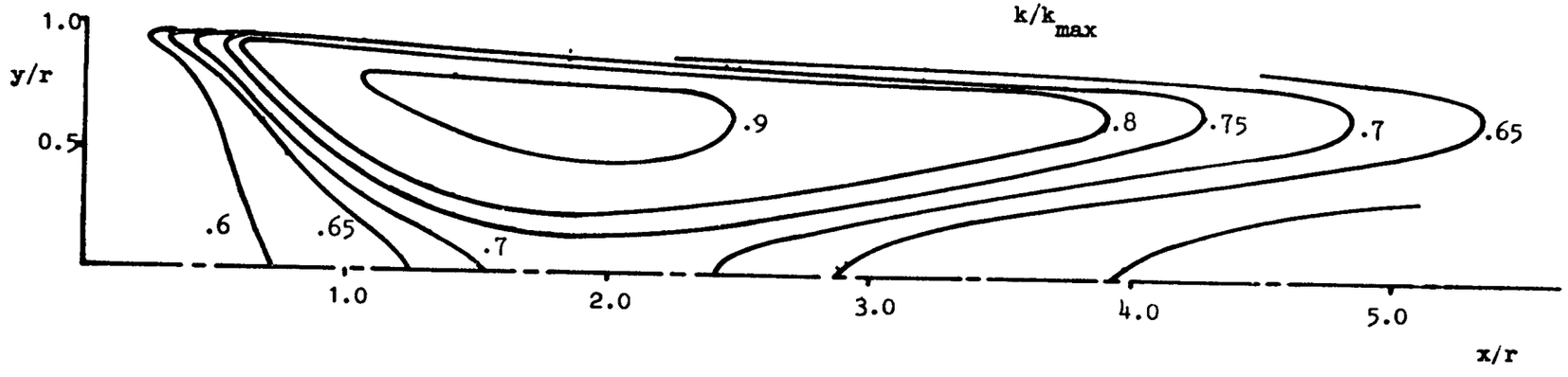


Fig. 6. Lines of equal turbulence kinetic energy in the wake.

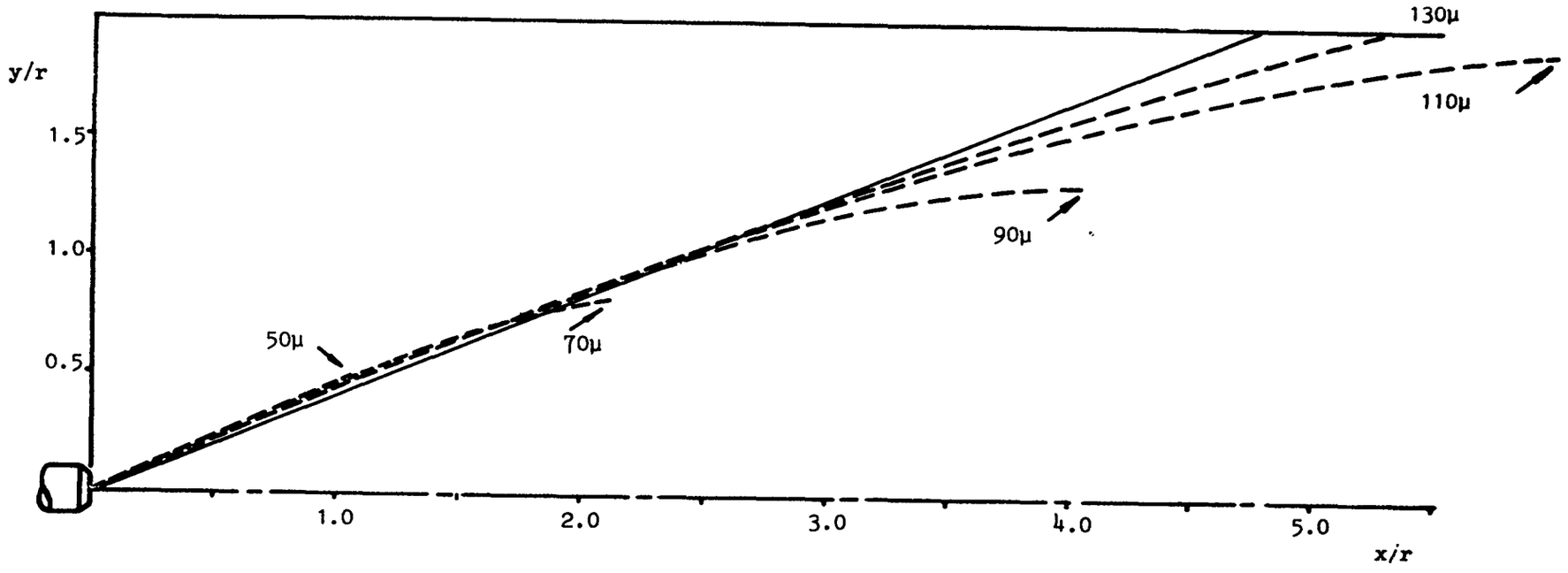


Fig. 7. Trajectories of ind·-idual droplets. Arrows indicate burnout locations. Solid line is the nominal cone.

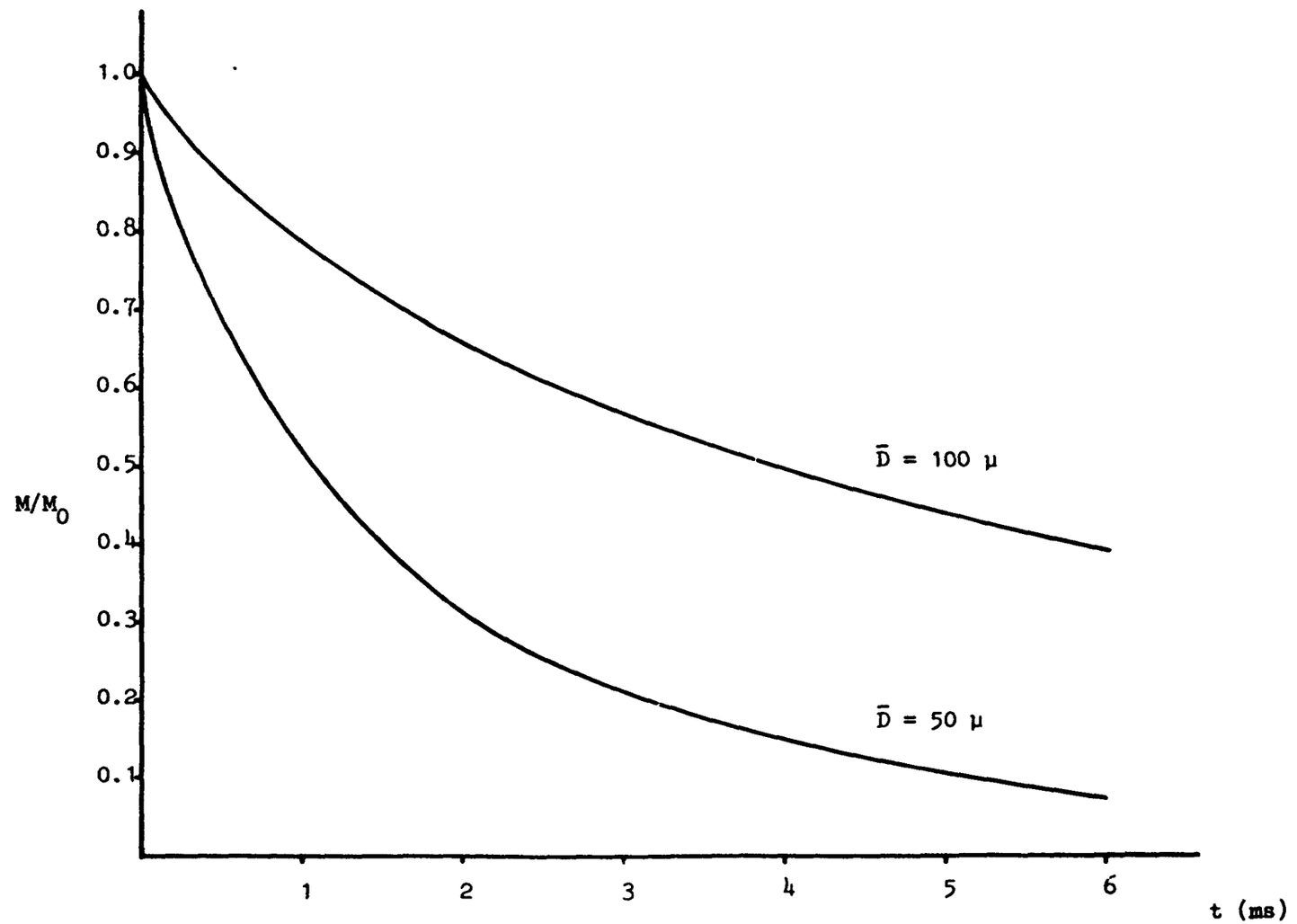


Fig. 8. Plots of unevaporated mass fraction against time, without forced convection ($\delta = 2$).

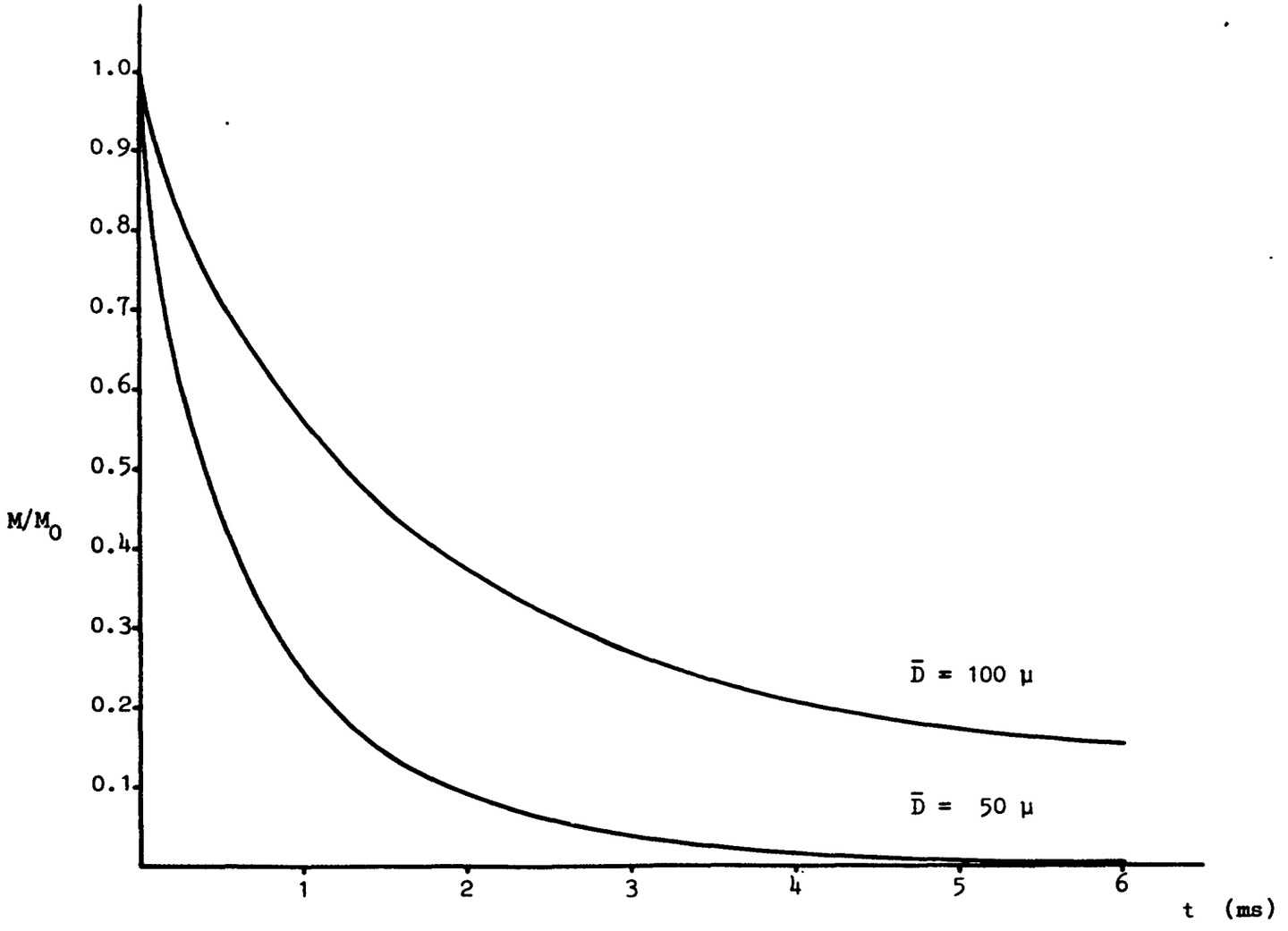


Fig. 9. Plots of unevaporated mass fraction against time, including forced convection ($\delta = 2$)

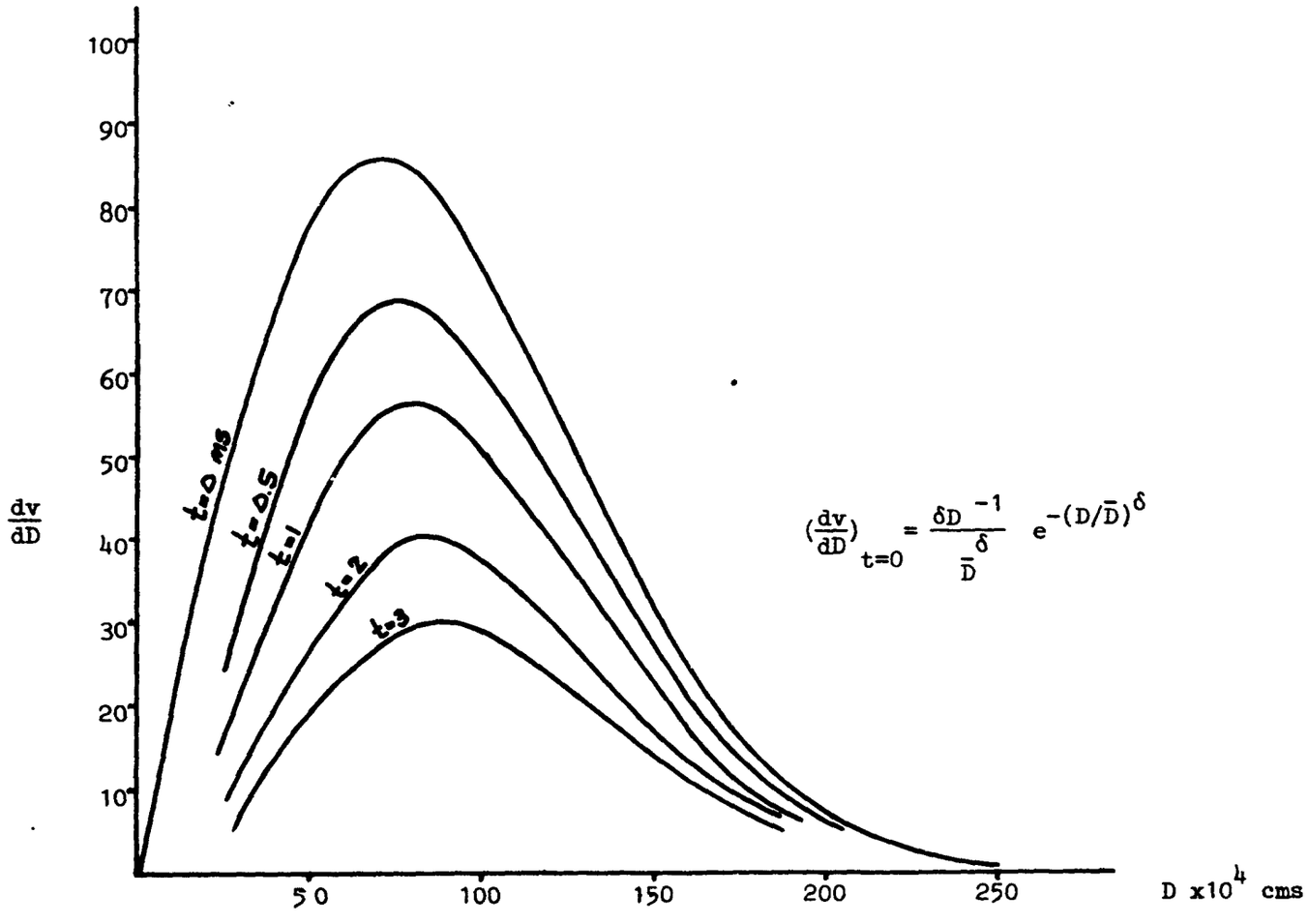


Fig. 10. The change of distribution function for size constant, $\bar{D}$ = 100 microns and distribution parameter $\delta$ = 2 at t = 0.

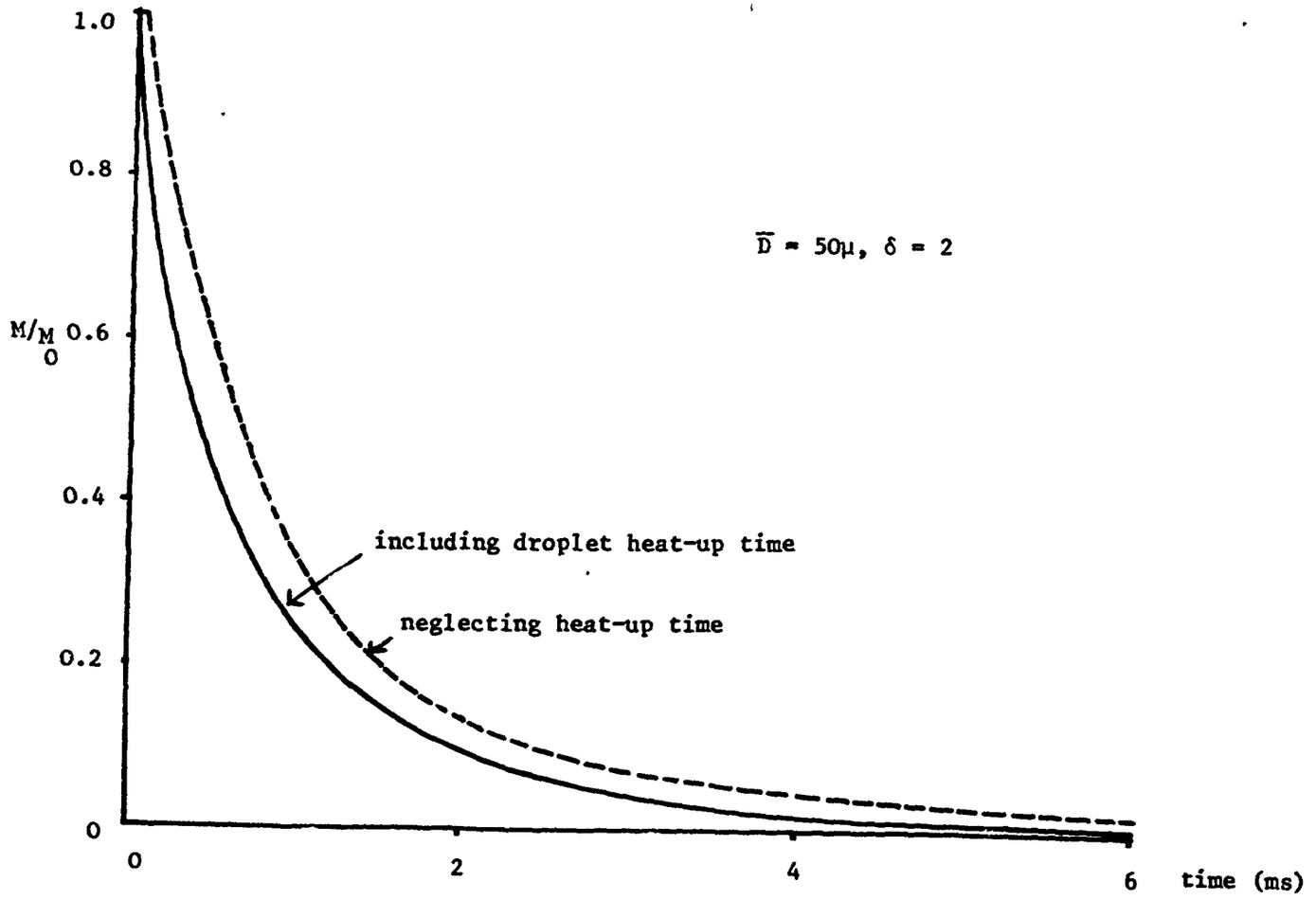


Fig. 11. Rate of evaporation with and without allowance for droplet heating up time.

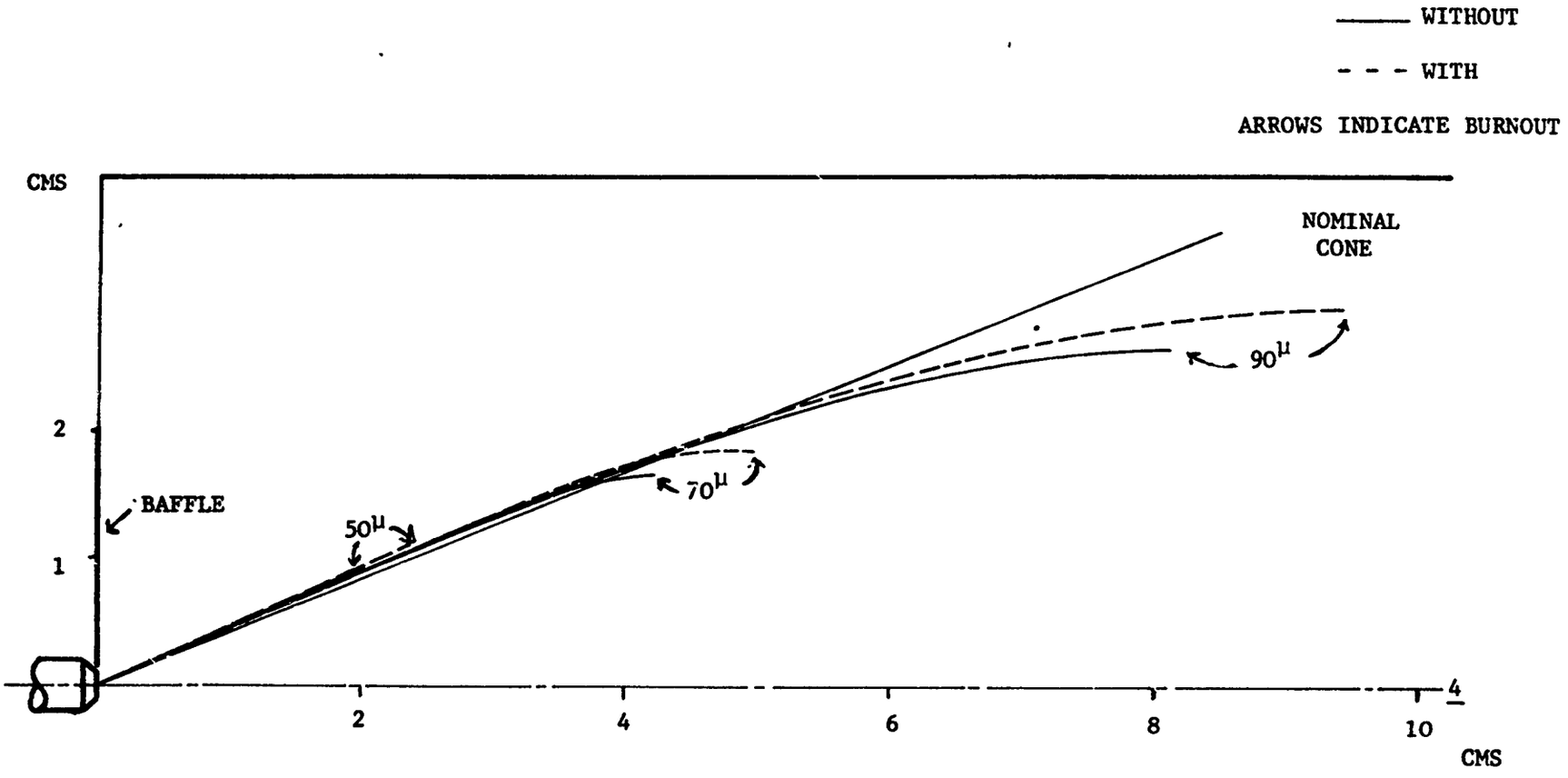


Fig. 12. Droplet trajectories with and without allowance for droplet heating-up time.

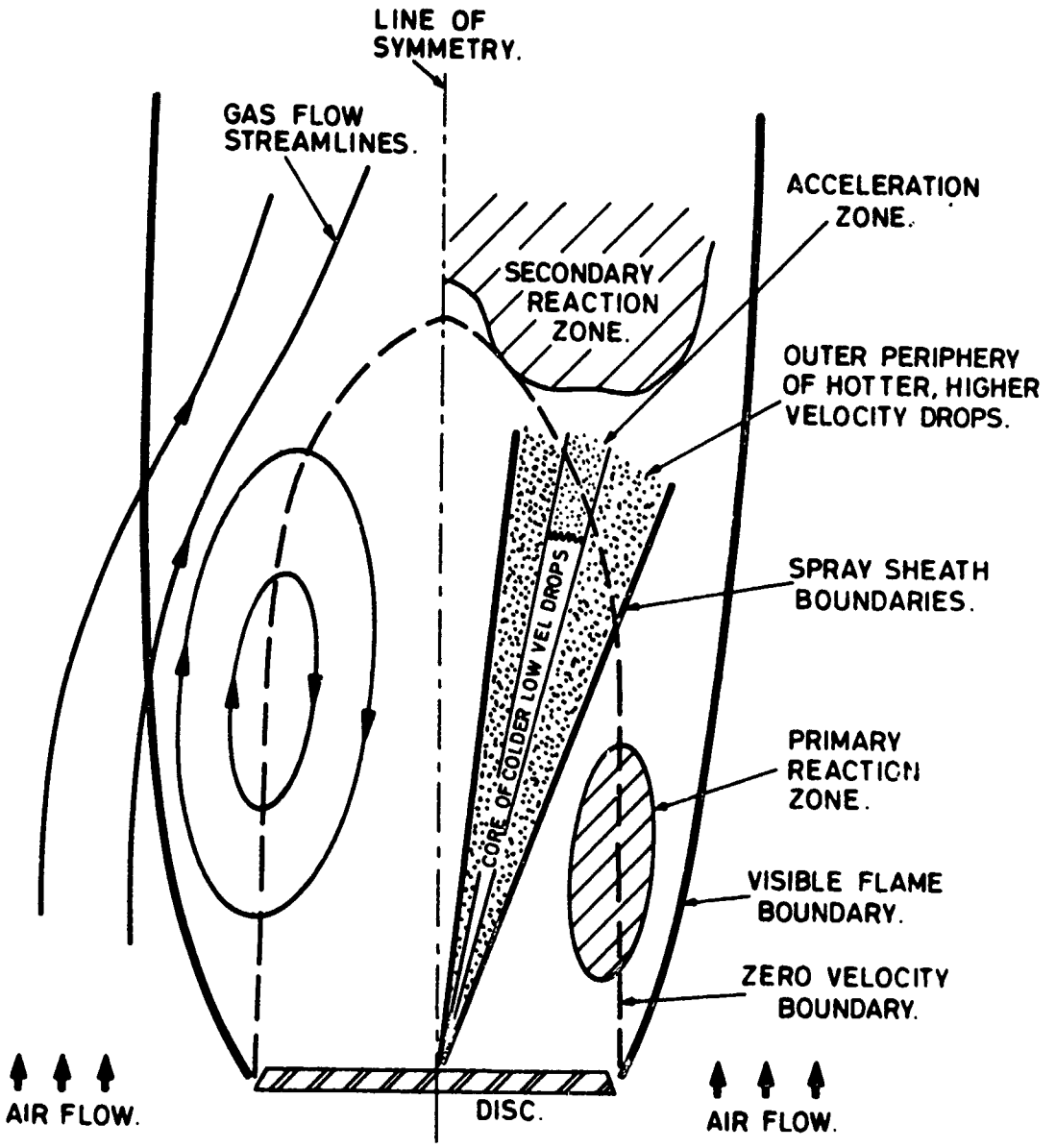


Fig. 13. Physical model of spray burning in the wake of a stabilizer disc[19].

SECURITY CLASSIFICATION OF THIS PAGE (When Data Entered)

| REPORT DOCUMENTATION PAGE | READ INSTRUCTIONS BEFORE COMPLETING FORM |
|---|---|
| 1. REPORT NUMBER: AFOSR-TR-78-0842 | 2. GOVT ACCESSION NO. / 3. RECIPIENT'S CATALOG NUMBER |
| 4. TITLE (and Subtitle): SPRAY EVAPORATION IN RECIRCULATING FLOW. | 5. TYPE OF REPORT & PERIOD COVERED: INTERIM rept. Mar 74 - Feb 78 |
| | 6. PERFORMING ORG. REPORT NUMBER: HIC-290 |
| 7. AUTHOR(s): F. BOYSON, J. SWITHENBANK | 8. CONTRACT OR GRANT NUMBER(s): AFOSR-74-2682 |
| 9. PERFORMING ORGANIZATION NAME AND ADDRESS: UNIVERSITY OF SHEFFIELD, CHEMICAL ENGINEERING & FUEL TECHNOLOGY DEPT, SHEFFIELD, S1 3JD. ENGLAND | 10. PROGRAM ELEMENT, PROJECT, TASK AREA & WORK UNIT NUMBERS: 2308A2, 61102F, A2 |
| 11. CONTROLLING OFFICE NAME AND ADDRESS: AIR FORCE OFFICE OF SCIENTIFIC RESEARCH/NA, BLDG 410, BOLLING AIR FORCE BASE, D C 20332 | 12. REPORT DATE: Apr 78 / 13. NUMBER OF PAGES: 39 (42p.) |
| 14. MONITORING AGENCY NAME & ADDRESS (if different from Controlling Office) | 15. SECURITY CLASS. (of this report): UNCLASSIFIED / 15a. DECLASSIFICATION/DOWNGRADING SCHEDULE |

16. DISTRIBUTION STATEMENT (of this Report)

Approved for public release; distribution unlimited.

17. DISTRIBUTION STATEMENT (of the abstract entered in Block 20, if different from Report)

18. SUPPLEMENTARY NOTES

19. KEY WORDS (Continue on reverse side if necessary and identify by block number)

MATHEMATICAL MODELLING
COMBUSTION
SPRAYS
EVAPORATION
ATOMIZATION

20. ABSTRACT (Continue on reverse side if necessary and identify by block number)

Since the overall rate of fuel evaporation in combustors is strongly influenced by the gas to drop relative velocity, detailed information on the aerodynamics of the flow in a given combustor configuration is essential for its prediction. Such aerodynamic information can be obtained either from measurements or mathematical simulation of events taking place in actual systems. Because of advances in mathematical modelling turbulent flow phenomena, and development of powerful techniques for solving the partial differential equations of fluid mechanics, the latter approach is becoming more efficient and economical. The flow equations can be solved using either 2-D or 3-D models; however, almost all

DD FORM 1 JAN 73 1473 EDITION OF 1 NOV 65 IS OBSOLETE

UNCLASSIFIED

SECURITY CLASSIFICATION OF THIS PAGE (When Data Entered)

400 047

practical systems may be treated as 2-D (axisymmetric) in the important region, which includes the region of soot formation near the fuel injector. The calculation procedures was here applied to the case of fuel injection into a recirculation zone behind a baffle in a duct. The elliptic flow equations were evaluated using the k, epsilon turbulence model. The results clearly demonstrated the controlling influence of the convective contribution to spray evaporation. For example, in conditions representative of combustion systems, the analysis indirectes the droplets have just deviated from their initial conical path towards the flow direction when they vanish. This phenomena is consistent with experimental observations and to a great extent justifies the use of two-dimensional modelling for the spray evaporation region of practical combustors.